Current Problems in Research

POPULAR SCIENTIST

Research Article

Nonlinear Dynamics of Skydiving with Variable Atmospheric Density and Gradual Parachute Deployment

Brandon Lee Kosaido[1,2], Kushendarsyah Saptaji[1], and Djati Wibowo[1]

[1] Department of Mechanical Engineering, Faculty of Engineering and Technology, Sampoerna University, Jakarta 12780, Indonesia
[2] Department of Aerospace & Mechanical Engineering, College of Engineering, University of Arizona, 1200 E University Blvd, Tucson, AZ 85721, United States of America
* Correspondence: Brandon Lee Kosaido (brandon.kosaido@my.sampoernauniversity.ac.id)

Citation

B. L. Kosaido, K. Saptaji, and D. Wibowo, "Nonlinear Dynamics of Skydiving with Variable Atmospheric Density and Gradual Parachute Deployment," *Current Problems in Research*, vol. 2, no. 2, pp. 20–34, 2026. doi: 10.70028/cpir.v2i2.109.

Article History

Received: 15 May 2026
Revised: 8 July 2026
Accepted: 29 July 2026
Published: 1 August 2026

Abstract

This study investigates the vertical motion of a skydiver under the influence of aerodynamic drag and variable atmospheric conditions. A mathematical model is developed based on Newton's second law, incorporating a quadratic drag force that depends on air density, velocity, drag coefficient, and reference area. Unlike simplified approaches, this study accounts for altitude-dependent air density using a standard atmospheric model, allowing for more realistic simulation of high-altitude descent. The transition between freefall and parachute deployment is modeled using a logistic function to represent gradual canopy inflation. The resulting nonlinear differential equations are solved numerically using the fourth-order Runge–Kutta (RK4) method. Simulation results show that aerodynamic drag plays a dominant role in limiting velocity, leading to the formation of terminal velocity during freefall and a significantly reduced steady-state velocity after parachute deployment. Additionally, the inclusion of variable air density improves the accuracy of velocity predictions, particularly at higher altitudes where density variations are significant. The findings demonstrate that combining aerodynamic modeling, atmospheric variation, and numerical methods provides a more comprehensive understanding of skydiving dynamics.

Keywords: Skydiving Dynamics, Aerodynamic Drag, Terminal Velocity, Atmospheric Model, Parachute Deployment.

1. Introduction

The concept of skydiving is first found by the Frenchman Andre-Jacques Garnerin at 1797 [1]. Despite it having existed from that era, skydiving still contains significant amount of risk. Earlier research in 1985 to 2005 indicates that the injury rate in civilian skydiving ranges from 140 to 174 and 0.85 and 7.7 fatalities for every 100000 jumps [2]. In recent data, the skydiving injury rate has decreased, where reports from the German, American, and British Parachute Associations evaluates 62 million jumps, which shows an average of 3200000 jumps per year with an average injury rate of 0.044% and an average fatality rate of 0.0011% [3]. Due to this, skydiving remains a high-risk activity. The injury in skydiving is typically because of human factors, where the incorrect flare maneuver, and hook turns, where experienced skydivers turn at lower heights, causing incorrect landing [4]. There's also a risk of skydiving deaths due to the parachute malfunctioning, which is rare contrary to popular belief [5].

The safety of skydiving is closely related to the control of aerodynamic forces acting on the body. Without sufficient aerodynamic drag, a falling body accelerates under gravity and reaches a high terminal velocity, leading to severe impact forces while landing [6]. With parachute, the wind resistance increases, causing the terminal velocity to lower significantly, which decreases the impact force while landing [7]. However, in deployment of the parachute, there are rare risks of Parachute Opening Shock (POS), where the force of the opening of the shock fractures or injures the body [8]. This is why safety procedures and improvements to the parachute mechanism keep evolving throughout the years, where the slider in parachute bag is invented to reduce the force of opening ram-air parachutes [9]. With all these factors in mind, the research is done to determine the forces working on the human body while skydiving, and how parachute deployment will affect the safety of freefall. Altitude will also be analyzed, as the wind density gets affected with different altitudes [10]. The report aims to make a simplified, yet realistic model, with different factors playing into skydiver using dynamics concept and numerical methods.

Different studies have brought into factor on how aerodynamic drag and altitude affects wind drag for skydivers. One such test is a wind tunnel simulation to simulate free-fall experiments. The skydiving has a nonlinear nature, with many factors such as body configurations, aerodynamic forces, and posture [11]. With the aerodynamics studies, the typical belly-to-earth position will give an air coefficient of 1.0 [11][12]. Studies using Computational Fluid Dynamics also examine how aircraft exit stage affect the wind flow of skydiver, where exiting the aircraft gives a significant amount of wind drag due to turbulence [13]. The aerodynamic drag paired with the thermodynamics are also reasons of skydiving distance limit, which is theoretically 45400 meters, although several factors decrease the maximum altitude significantly [14]. Studies have simplified the forces to vertical forces, where the wind drag and body mass are the significant forces acting on the skydiver [15].

The altitude affects wind density, causing the drag force to change with the altitude. Research from AIAA and Simene simulates aircrafts at different atmospheric heights, where it concludes that each atmosphere layer will decrease air density at higher heights [16], [17]. The physical reason is the decrease in gravity at higher heights, causing less air pressure, which will decrease the density of air [18]. Another study proves this, where different people are tested to do activities above 6000 feet. The studies states that the deep, rapid breathing, added with exhaustion at performing simple tasks, due to the lack of oxygen in higher altitudes [19].

RK4 Method is used to calculate the next parameters on time. Due to the nonlinear nature of the equations, RK4 is applied to solve the nonlinear equations from the varying aerodynamics drag and atmospheric density. Studies have attempted to solve velocity-squared drag projectile motion with analytical method, but the nonlinearities proved to be difficult to solve analytically [20]. As a result, RK4 method is utilized to compute velocity and displacement with high accuracy with the actual data, even with asymmetric trajectories. RK4 has also been refined using contra-harmonic averaging approach, where each constant of RK4 is averaged to improve accuracy on a numerical method that is known for its accuracy, showing that improvements on accuracy is possible for RK4 [21]. With these considerations, this study aims to analyze the influence of altitude and parachute area on velocity, acceleration, and descent behavior during freefall and parachute deployment. To achieve this, the objectives are: (1) to develop a numerical skydiving model that incorporates nonlinear aerodynamic drag, variable atmospheric density, and gradual parachute deployment, solved using the RK4 method; and (2) to compare the resulting model predictions with real-world skydiving data to assess the accuracy of a one-dimensional nonlinear motion model in simulating freefall.

2. Materials and Methods

This study develops a physics-based model of the vertical motion of a skydiver subjected to aerodynamic drag under varying atmospheric conditions, based on a free-body analysis and Newton's second law. The implementation is done using MATLAB, where the governing equations of time (t), height (h), using the altitude-dependent density ($\boldsymbol{\rho}$) are solved for velocity (v) and height (h) using the RK4 method. There are few assumptions that are done to simplify the analysis while maintaining physical relevance, several assumptions are made. First, the altitude range considered is assumed to span the troposphere to the lower stratosphere, approximately 3–12 km (10,000–40,000 ft), consistent with typical skydiving deployment altitudes of 10,000–15,000 ft and HALO (High Altitude Low Opening) jumps of 5–12 km [22], [23]. Another assumption is a stable vertical motion on the parachute, to focus on the dominating vertical force that wind creates on sky-fall. The parachute inflation process is also assumed to inflate symmetrically, using the logistic function. The mass of the human body is 80 kg [24], according to the average human weight. The drag coefficients are 1.0 for human body [25], and 1.5 for the parachute [26], according to studies on parachute aerodynamics. The frontal area of human body is approximately 0.7 m^2, and 25 m^2 for the parachute. The initial deployment altitude will be done at 5000 and 20000 meters respectively. Then, the parachute will be deployed at the height of 500 m.

2.1. Equation of motion

2.1.1 Equation of air density

Since the height is between the lower stratosphere and troposphere, using the NASA's atmospheric model [27], the air pressure in troposphere, with the assumption of Hydrostatic equilibrium and Ideal Gas, is as follows

$$T(h) = T_0 - 0.0065h \tag{1}$$

$$P = P_0 \left(\frac{T(h) + 273.15}{T_0 + 273.15} \right)^{\frac{Mg}{RL}} \tag{2}$$

Where $\boldsymbol{P_0}$ is the initial pressure of 101.29 Kpa, the g is the acceleration of gravity, $\boldsymbol{T}$ is the temperature, where the initial temperature $\boldsymbol{T_0}$ is 15.04° C, M is the molar mass of air calculated to be 0.028694 $\frac{kg}{mol}$, R is the Ideal Gas constant, which is 8.314 $\frac{J}{mol \cdot K}$, and $\boldsymbol{L}$ is a temperature lapse rate, which is approximated to be 0.0065 K/m. As for the lower stratosphere, the air pressure is finalized to be

$$P = 22.65 \cdot e^{1.73 - 0.000157h} \tag{3}$$

Using this Pressure, we can determine the air density.

$$\rho = \frac{P(h)}{0.2869 \cdot (T(h) + 273.15)} \tag{4}$$

2.1.2 Logistic Function

As for the parachute the inflation is done using the logistic function, due to the assumption that the parachute inflates symmetrically.

$$f_{inflation} = 1 - e^{-\frac{t_{inflation} - t_{time\ of\ stretch}}{\tau_{inflation}}} \tag{5}$$

Where $\tau_{inflation}$ is the constant controlling the speed of inflation, valued at 0.8 seconds, and the $t_{inflation}$ is the time of parachute inflation. Deployment is modelled in two stages: a 0.5 second line-stretch delay during which no drag-area increase occurs, followed by logistic inflation phase described in equation 5. The $f_{inflation}$ is a dimensionless unit and ranges from 0 to 1, representing the fraction of full canopy inflation at time t. The model is derived by logistic function, where it is used for the growth of the size of the parachute, assuming it opens symmetrically [28].

2.1.3 Free-body diagram analysis

The free-body diagram of a skydiver with no parachute can be shown in Figure 1.

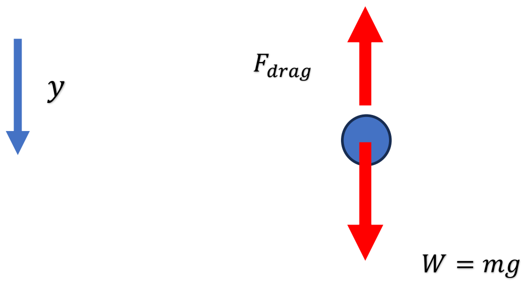

Figure 1. 1D free-body diagram of a skydiver, with and without parachute

Using the Newton's 2nd law, we can determine the acceleration of the forces at the skydiver.

$$\Sigma F_y = m \cdot a \tag{6}$$

$$m \cdot a = W - F_{drag} \tag{7}$$

Where F_{drag} is the air drag force, which is found by:

$$F_{drag} = \frac{1}{2} C_d A \rho(h) v^2 \tag{8}$$

Where C_d is the coefficient of drag, A is the reference area, $\rho(h)$ is the altitude-dependent air density from Equation 4, and v is the instantaneous descent velocity. The acceleration can be derived as $\frac{dv}{dt}$ to be used in the RK4 numerical method.

$$a = \frac{dv}{dt} = g - \frac{1}{2m} C_d A \rho(h) v^2 \tag{9}$$

Similarly, knowing the velocity is displacement in respect to time, we can find the differential equation of:

$$\frac{dh}{dt} = v \tag{10}$$

At the state of parachute inflation, the FBD is shown in Figure 2.

https://doi.org/10.70028/cpir.v2i2.109

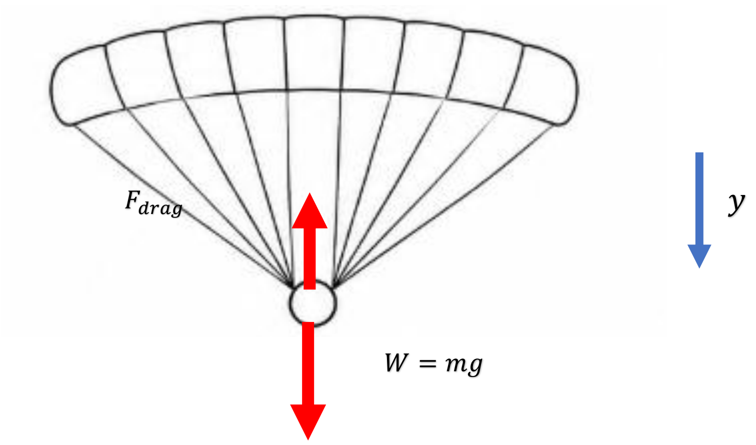

Figure 2. 1D Free-Body Diagram of a skydiver with parachute

According to Newton's 2nd law, the acceleration can be determined by finding the same forces.

$$\Sigma F_y = ma \quad (11)$$

$$ma = W - F_{drag} \quad (12)$$

$$ma = mg - \frac{1}{2} C_d A \rho(h) v^2 \quad (13)$$

During deployment, the total drag force is modeled as the superposition of the drag force generated by the human body and the drag force generated by the parachute canopy, weighted by the inflation fraction. Since drag force scales with the product of the drag coefficient and reference area rather than with each quantity separately, this study defines a combined drag-area term as a linear blend of the human-body and parachute drag-area products, rather than blending the drag coefficient and area separately. This is a modeling assumption of this study, representing a first-order approximation of the added-drag transition during gradual canopy deployment, and is expressed as follows.

$$f_{inflation} = 1 - e^{-\frac{t_{inflation} - t_{time\ stretch}}{\tau_{inflation}}} \quad (14)$$

$$(C_d A)_{total} = (C_d A)_{human} + f_{inflation} \cdot (C_d A)_{parachute} \quad (15)$$

Rest of the differential equation is similar to the first state, which is as follows.

$$a = \frac{dv}{dt} = g - \frac{1}{2m} (C_d A)_{total} \rho(h) v^2 \quad (16)$$

$$v = \frac{dh}{dt} \quad (17)$$

2.1.4 RK4 Method

Using the RK4, with the time step being 0.05 seconds and 300 seconds simulation times, we can compute the RK4 method to numerically integrate the velocity at the next loop. Both of these RK4 method will be applied on both states. RK4 is typically solved for linear differential equations, which can determine the next state of velocity and height for parachute skydiving [30].

$$v_{n+1} = v_n + \frac{1}{6}(k_{1v} + 2k_{2v} + 2k_{3v} + k_{4v}) \tag{18}$$

$$h_{n+1} = h_n + \frac{1}{6}(k_{1h} + 2k_{2h} + 2k_{3h} + k_{4h}) \tag{19}$$

$$Solving\ for\ k_1$$

$$k_{1,V} = \Delta t\left(\frac{dv}{dt}(t, v, h)\right) = \Delta t \cdot \left(g - \frac{(C_d A\rho(h)v^2}{2m}\right) \tag{20}$$

$$k_{1,h} = \Delta t\left(\frac{dh}{dt}(t, v, h)\right) = \Delta t \cdot (v) \tag{21}$$

$$Solving\ for\ k_2$$

$$k_{2,v} = \Delta t\left(\frac{dv}{dt}\left(t + \frac{\Delta t}{2}, v + \frac{k_{1v}}{2}, h + \frac{k_{1h}}{2}\right)\right) \tag{22}$$

$$k_{2,v} = \Delta t\left(\frac{dv}{dt}\left(t + \frac{\Delta t}{2}, v + \frac{k_{1v}}{2}, h + \frac{k_{1h}}{2}\right)\right) \tag{23}$$

$$k_{2,h} = \Delta t\left(\frac{dh}{dt}\left(t + \frac{\Delta t}{2}, v + \frac{k_{1v}}{2}, h + \frac{k_{1h}}{2}\right)\right) = \Delta t\left(v + \frac{k_{1v}}{2}\right) \tag{24}$$

$$Solving\ for\ k_3$$

$$k_{3,v} = \Delta t\left(\frac{dv}{dt}\left(t + \frac{\Delta t}{2}, v + \frac{k_{2v}}{2}, h + \frac{k_{2h}}{2}\right)\right) \tag{25}$$

$$k_{3,v} = \Delta t\left(g - \frac{C_d A\rho\left(h + \frac{k_{2h}}{2}\right)\left(v + \frac{k_{2v}}{2}\right)^2}{2m}\right) \tag{26}$$

$$k_{3,h} = \Delta t\left(\frac{dh}{dt}\left(t + \frac{\Delta t}{2}, v + \frac{k_{2v}}{2}, h + \frac{k_{2h}}{2}\right)\right) = \Delta t\left(v + \frac{k_{2v}}{2}\right) \tag{27}$$

$$Solving\ for\ k_4$$

$$k_{4,v} = \Delta t\left(\frac{dv}{dt}(t + \Delta t, v + k_{3v}, h + k_{3h})\right) \tag{28}$$

$$k_{4,v} = \Delta t\left(g - \frac{C_d A\rho(h + k_{3h})(v + k_{3v})^2}{2m}\right) \tag{29}$$

$$k_{4,h} = \Delta t\left(\frac{dh}{dt}(t + \Delta t, v + k_{3v}, h + k_{3h})\right) = \Delta t(v + k_{3v}) \tag{30}$$

After defining each parameter and equations, the simulation is done. The simulation begins by defining initial conditions and system parameters, including mass, drag coefficient, and reference area. Arrays are initialized to store time-dependent variables such as velocity and altitude. At each step, atmospheric properties are updated based on the current altitude. The governing equations are then solved using the RK4 method to obtain the system's state in the next iteration. Then, the results are visualized through plots of velocity and altitude as functions of time, providing insight into the aerodynamic behavior of the system. The parameters that are utilized are position (h), velocity (v), and acceleration (a) of skydiver. The impact velocity and terminal velocity are also compared to the actual data of skydiving terminal velocity. In addition, the parachute area will follow based on real parachute, where 15 m^2, 25 m^2, and 33 m^2, following the area of Opale Rescue Parachute, Ultra Cross 100, and Sky Country SQ-33 Parachute respectively. The schematics on Figure 3 show the rough sketch on the parachute canopy area.

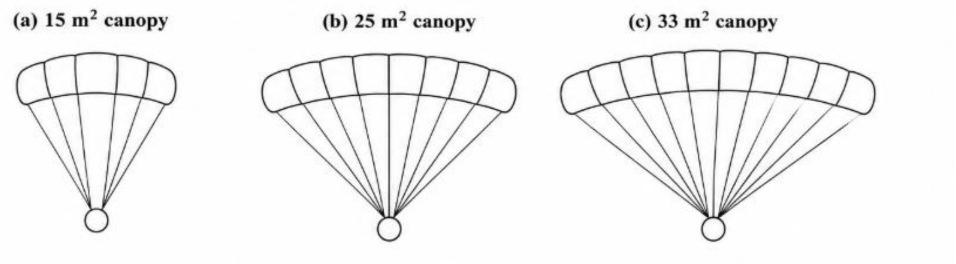

Figure 3. Representative schematics of parachute canopy models used for the parametric study

3. Results and Discussion

Before presenting the simulation results, the numerical implementation procedure is summarized below. At each time step, the atmospheric density is first computed from the current altitude using the model described in Eq. (1)–(4). The parachute deployment state is then checked against the deployment altitude: if the parachute has not yet been deployed, the drag-area term uses only the human-body contribution; otherwise, the inflation fraction is computed from the logistic function (Eq. 5) and the combined drag-area term is updated accordingly (Eq. 8). The RK4 method is then applied to advance velocity and height to the next time step. This procedure repeats until the skydiver reaches ground level (h = 0) or the simulation time limit is reached. The complete procedure is given in Algorithm 1.

```
Input: m, g, Cd_human, A_human, Cd_parachute, A_parachute,
τ_inflation, deploy_altitude, h0, Δt, t_end
Output: v(t), h(t), a(t), impact velocity

t ← 0, v ← 0, h ← h0
while t < t_end and h > 0 do
    ρ ← compute air density at h                  ▷ Eq. (1)-(4)
    if h <= deploy_altitude then
        f_inflation ← 1 - exp(-(t - t_deploy)/τ_inflation)     ▷ Eq. (5)
        (CdA)_total ← (CdA)_human + f_inflation · (CdA)_parachute   ▷ Eq. (8)
    else
```

```
        (CdA)_total ← (CdA)_human
    end if
    k1_v ← Δt · [g - (CdA)_total·ρ·v² / (2m)]
    k1_h ← Δt · v
    k2_v ← Δt · [g - (CdA)_total·ρ·(v + k1_v/2)² / (2m)]
    k2_h ← Δt · (v + k1_v/2)
    k3_v ← Δt · [g - (CdA)_total·ρ·(v + k2_v/2)² / (2m)]
    k3_h ← Δt · (v + k2_v/2)
    k4_v ← Δt · [g - (CdA)_total·ρ·(v + k3_v)² / (2m)]
    k4_h ← Δt · (v + k3_v)
    v ← v + (k1_v + 2k2_v + 2k3_v + k4_v) / 6
    h ← h + (k1_h + 2k2_h + 2k3_h + k4_h) / 6
    store v, h, a, t
    t ← t + Δt
end while
return v(t), h(t), a(t), v at h = 0
```

Algorithm 1. Pseudocode of the MATLAB Simulation

The simulation parameters used across all scenarios are summarized in Table 1. These values remain fixed across the parametric study, with only the parachute area and atmospheric layer varied between scenarios to examine their effect on descent behavior.

Table 1. Initial Parameters defined for simulation

No.	Parameter	Symbol	Value	Unit
1.	Skydiver mass	m	80	Kg
2.	Gravitational acceleration	g	9.81	m/s^2
3.	Human drag coefficient	Cd_human	1.0	-
4.	Parachute drag coefficient	Cd_parachute	1.5	-
5.	Human frontal area	A_human	0.7	m^2
6.	Parachute canopy area (varied)	A_parachute	15, 25, 33	m^2
7.	Initial altitude — Troposphere case	h0	5000	m
8	Initial altitude — Lower Stratosphere case	h0	20000	m
9	Parachute deployment altitude	deployment_altitude	500	M
10	Line-stretch time	line_stretch_time	0.5	s
11	Inflation time constant	τ_inflation	0.8	s

https://doi.org/10.70028/cpir.v2i2.109

12	Time step	Δt	0.05	s
13	Total simulation time	t_final	3000	s
14	Sea-level reference pressure	P_0	101.325	kPa
15	Sea-level reference temperature	T_0	15.04	$°C$
16	Stratosphere base pressure coefficient	–	22.65	kPa

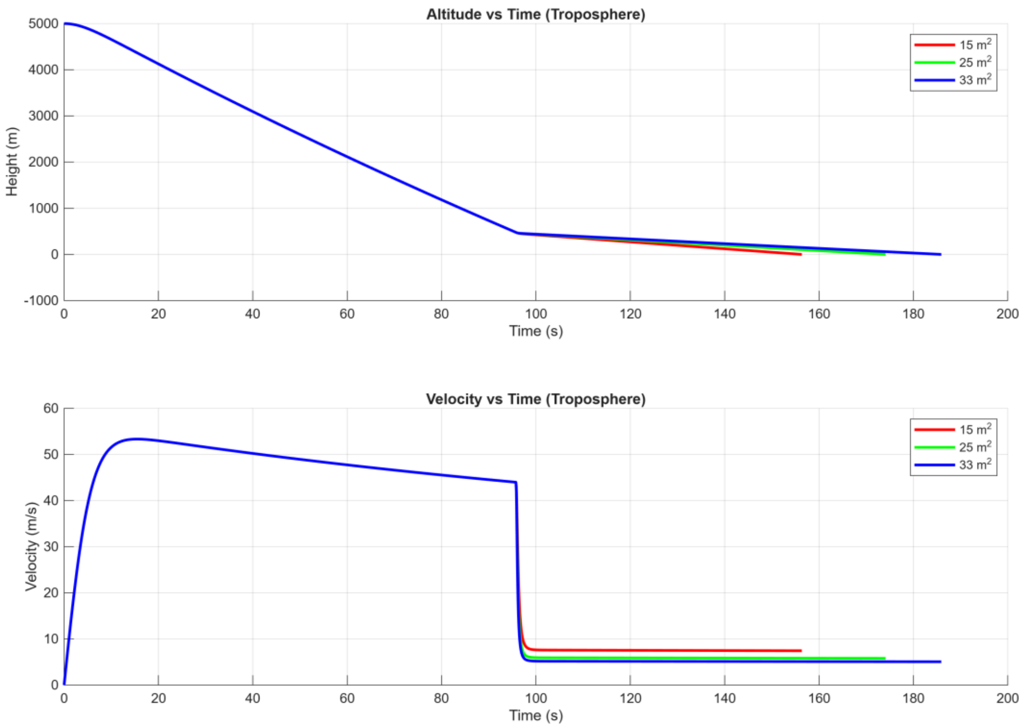

Figure 4. Altitude and Velocity graph of Troposphere distance

Figure 4 shows three distinct phases. In Phase 1 of freefall, velocity increases rapidly from 0 as gravity dominates over the small aerodynamic drag force, making altitude decreases at an accelerating rate. In this phase, the drag that scales with v^2 is negligible at lower speed. In Phase 2, drag grows quadratically with velocity until it approaches gravitational force, and velocity asymptotically approaches terminal velocity. This causes the altitude to decrease at a nearly constant, maximum rate. In Phase 3, following parachute deployment, the sudden increase in effective drag area and coefficient causes a sharp deceleration, after which velocity settles into a new, much lower steady descent rate (~40 m/s in this scenario) as drag once again balances gravity at the new, larger effective drag area.

https://doi.org/10.70028/cpir.v2i2.109

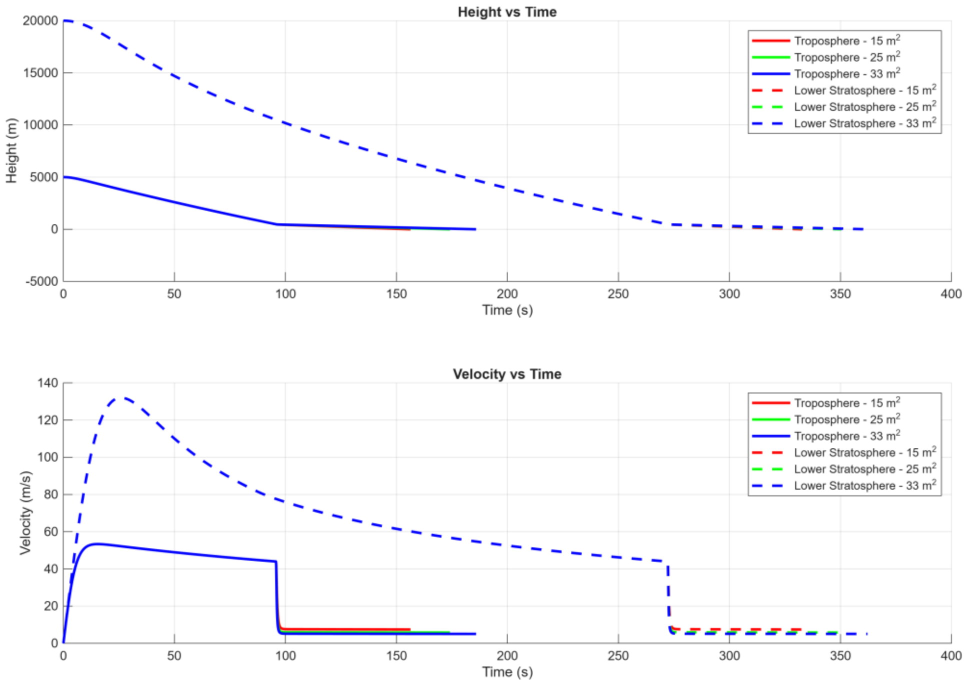

Figure 5. Comparison Altitude and Velocity graph between troposphere and lower Stratosphere

In Figure 5, it shows that in lower stratosphere levels, The decrease is more significant compared to the troposphere. This is due to the air density being lower in those heights, causing it to decrease significantly until position of 11000 km, where it decreases with less spike, following the stratosphere trend. The terminal or maximum velocity is calculated to be 132.00 m/s, which is close to the range of the lower stratosphere terminal velocity. The higher heights make it take more time for the altitude to go to 0, which is why the decrease is steeper than the troposphere.

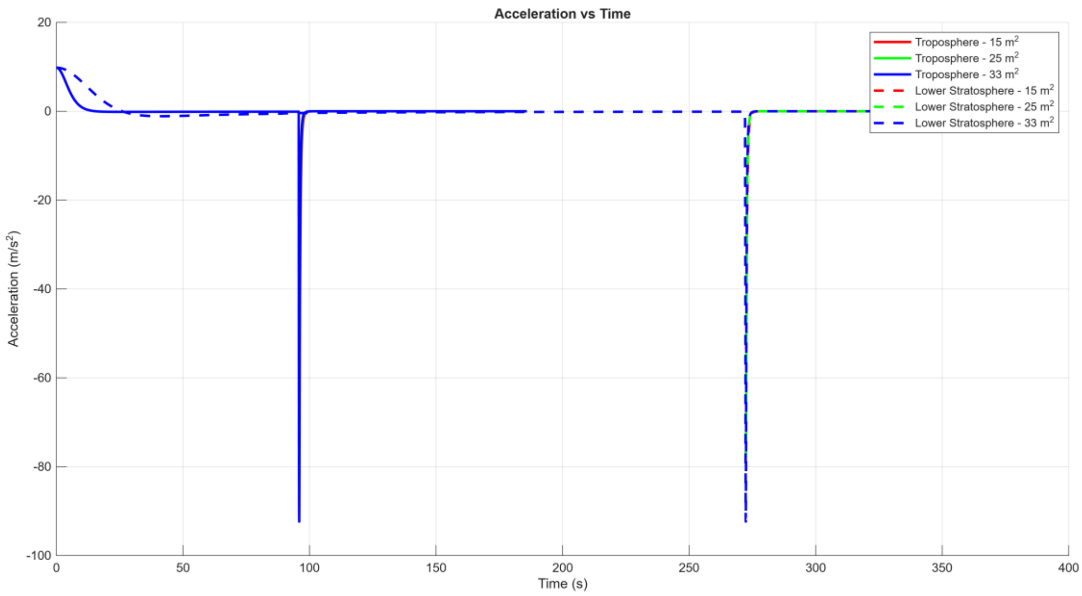

Figure 6. Acceleration graph comparison between atmospheres and parachute area

For the acceleration, Figure 6 shows that the acceleration was initially at the dropoff position, until it reaches terminal velocity until it decreases due to the maximum air drag force being at its maximum. As such, the graph shows that starts from positive, to small negative, then increase to 0. At the parachute deployment, the acceleration has a low spike, due to the parachute opening significantly decreasing the velocity. The average velocity is counted to be 5.33 m/s, which is still in range of 5-7 m/s parachute fall speed [32].

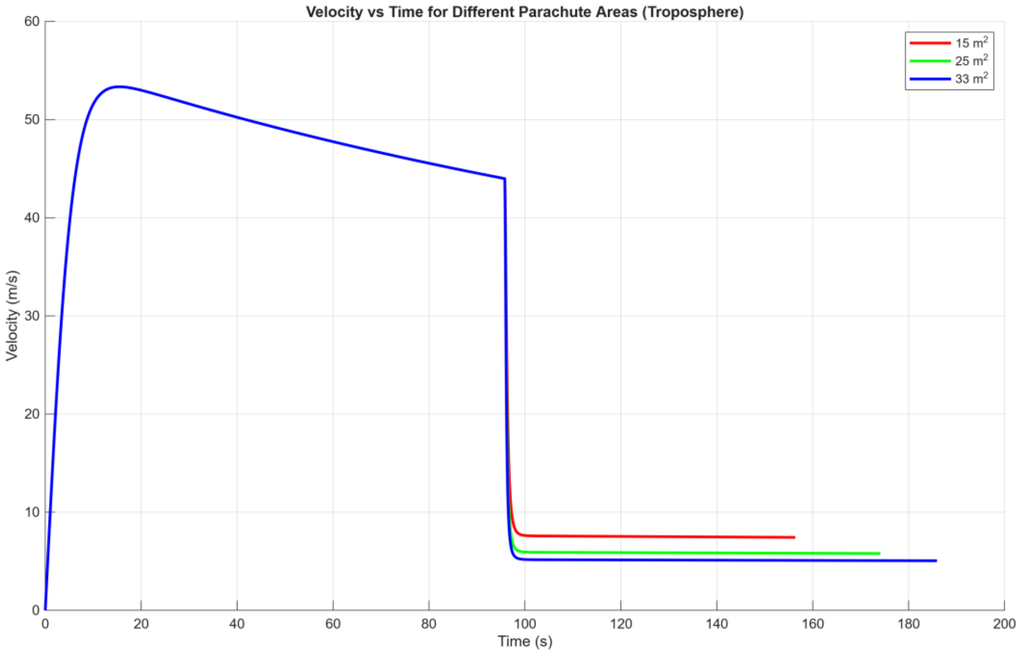

Figure 7. Velocity graph with different Parachute area

Figure 7 is shown to determine if the difference between the parachute area will affect the terminal velocity of the skyfall. It shows that the smaller area of parachute will give higher impact velocity, shown by the 15 m^2 parachute area will give the impact velocity of 6.99 m/s. While this speed is safe, it still has a chance to give injury on skydiver. The 25 and 33 m^2 parachute area gives impact velocity of 5.41 m/s and 5.05 m/s respectively, which are the safer impact velocities that have less chance of injuries [13]. Compiling each data of height and parachute area, the data are shown in Table 2.

Table 2. Impact and Max Velocity on Parachute area and atmosphere layer

No.	Atmosphere	Area (m²)	Parachute Model	Max Velocity (m/s)	Impact Velocity (m/s)	Calculated impact velocity	Percentage discrepancy (%)
1.	Troposphere	15	Opale Rescue Parachute [33]	53.34	7.43	7.55	1.615
2.	Troposphere	25	Ultra Cross 100 [34]	53.34	5.79	5	15.8
3.	Troposphere	33	Sky Country SQ-33 Parachute [35]	53.34	5.05	4.93	2.434
4.	Lower Stratosphere	15	Opale Rescue	132	7.43	7.55	1.615

5.	Lower Stratosphere	25	Parachute [33] Ultra Cross 100 [34]	132	5.79	5	15.8
6.	Lower Stratosphere	33	Sky Country SQ-33 Parachute [35]	132	5.05	4.93	2.434

Table 2 shows that altitude affects terminal velocity, while parachute area affects the impact velocity. The simulations indicate that jumps performed in the lower stratosphere produce higher max velocity at 132 m/s. This is due to the lower density of air, causing less resistance and higher velocity at lower stratospheric height. The troposphere is significantly lower at 53.34 m/s, due to higher air drag at lower altitudes. The expected value of terminal velocity in troposphere is 55 m/s, which is defined by equation 17 [36].

$$V_t = \sqrt{\frac{2mg}{\rho A C_d}} \tag{31}$$

The expected impact velocity calculated using equation 17 is also quite similar from the calculations and the expected value. From Table 2, the discrepancy of calculated impact velocity value and the simulated value on 15 and 33 m^2 area is small at 1.615 and 2.434 percent. However, the 25 m^2 area has highest discrepancy of 15.8%. This means that while the model is accurate on most parachute areas, there are some room for improvements. In addition, the referenced parachute in the manuscript might also represent different drag coefficients than the single constant assumed in this model. Improvement's suggestions is doing aerodynamic model using CFD, or apply horizontal forces and more realistic parachute opening model, and find individual drag coefficient on each referenced parachute or parachute area.

4. Conclusions

This study presents a numerical analysis of vertical motion under aerodynamic drag using a variable air density model. By incorporating atmospheric variations and nonlinear drag effects, the simulation provides a more realistic representation of the system's dynamic behavior compared to constant-density assumptions. The results demonstrate that aerodynamic drag plays a dominant role in governing both velocity and displacement. Prior to the increase in drag area, the system experiences rapid acceleration and higher descent velocity. However, as aerodynamic resistance increases, a significant reduction in velocity is observed, leading to a lower terminal condition. The influence of air density variation further enhances this effect, as increasing density at lower altitudes contributes to additional deceleration. In addition, the increase in area parachute also increases the aerodynamic drag, causing higher resistance. The application of a RK4 method enables accurate numerical integration of the governing equations, ensuring stable and reliable results throughout the simulation. The model successfully captures both transient and steady-state responses, highlighting the importance of coupling aerodynamic forces with atmospheric conditions. Despite the effectiveness of the model, several limitations remain. The analysis assumes purely vertical motion and neglects horizontal wind effects, which may influence real-world behavior. Additionally, simplifications in aerodynamic modelling may limit accuracy under complex flow conditions. Future work may include extending the model to two-dimensional motion, incorporating more detailed aerodynamic coefficients, and validating the results through experimental test.

https://doi.org/10.70028/cpir.v2i2.109

Acknowledgements

The authors would like to thank the Department of Mechanical Engineering, Sampoerna University, for providing the facilities and support for this research.

Funding

This study was not supported by any grants from funding bodies in the public, private, or not-for-profit sectors.

Conflict of Interest

The authors declare no conflicts of interest

Generative AI Declarations

Not Applicable.

Author Contributions

Brandon Lee Kosaido: Writing—Review and Editing, Methodology, Investigation, Software. Kushendarsyah Saptaji: Conceptualization, Writing—Review and Editing, Supervision. Djati Wibowo: Writing—Review and Editing, Supervision, Conceptualization. All authors have read and agreed to the published version of the manuscript.

Availability of Data and Materials

The datasets generated and/or analysed during the current study are available from the corresponding author on reasonable request.

Abbreviations

The following abbreviations are used in this manuscript:

RK4	Runge-Kutta 4

References

[1] B. Worth, "History and evolution of competitive body flight," in *Proceedings of the 8th Aerodynamic Decelerator and Balloon Technology Conference*., Hyannis, MA, USA, Apr. 1984, doi: 10.2514/6.1984-830.

[2] M. Damhuis, R. van der Wal, H. Frielink, R. Nijveldt, J. ten Brinke, and E. Tan, "The ground is the limit: epidemiology of skydiving accidents over 25 years and in 2.1 million jumps in the Netherlands with sub-analysis of injuries reported by medical professionals in the past five years," *World Journal of Emergency Surgery*., vol. 19, no. 1, p. 7, Dec. 2024, doi: 10.1186/S13017-024-00535-W.

[3] C. Barthel, S. Halvachizadeh, J. G. Gamble, H. C. Pape, and T. Rauer, " Recreational skydiving—Really that dangerous? A systematic review," *International Journal of Environmental Research and Public Health*, vol. 20, no. 2, p. 1254, Jan. 2023, doi: 10.3390/ijerph20021254.

[4] D. Doroftei et al., "FORENSIC ASPECTS OF SKYDIVING-RELATED DEATHS AND INJURIES," *Romanian Journal of Legal Medicine*, vol. 30, no. 4, pp. 258–263, Dec. 2022, doi: 10.4323/rjlm.2022.258.

[5] F. Mele, G. Mandarelli, G. Bottari, and B. Solarino, "Parachuting fatality: A case report video-recorded," *Forensic Science International: Reports*, vol. 4, p. 100220, Nov. 2021, doi: 10.1016/J.FSIR.2021.100220.

[6] R. W. Yeh et al., "Parachute use to prevent death and major trauma when jumping from aircraft: randomized controlled trial," *BMJ*, vol. 363, 2018, doi: 10.1136/BMJ.K5094.

[7] K. Gladh, R. Lo Martire, B. O. äng, P. Lindholm, J. Nilsson, and A. Westman, "Decelerations of parachute opening shock in skydivers," *Aerospace Medicine and Human Performance*., vol. 88, no. 2, pp. 121–127, Feb. 2017, doi: 10.3357/AMHP.4731.2017.

[8] J. Lazzari et al., “Pelvic fractures and Parachute Opening Shock (POS): Unveiling a rare skydiving Hazard. A case study and systematic review of the literature,” *Legal Medicine*., vol. 75, May 2025, doi: 10.1016/j.legalmed.2025.102629.

[9] [9] A. Westman, "Dangers in sport parachuting," Ph.D. dissertation, Department of Surgical and Perioperative Sciences, Umeå University., Umeå, Sweden, 2009. [Online]. Available: http://urn.kb.se/resolve?urn=urn:nbn:se:umu:diva-19690.

[10] Y. C. He, H. B. Lin, J. Y. Fu, P. W. Chan, Q. X. Zheng, and T. Deng, “Dependence of wind load on air density for highrise buildings,” *Journal of Wind Engineering and Industrial Aerodynamics*, vol. 211, p. 104558, Apr. 2021, doi: 10.1016/j.jweia.2021.104558.

[11] A. Clarke and P.-O. Gutman, “A dynamic model of a skydiver with validation in wind tunnel and free fall,” *IFAC Journal of Systems and Control*, vol. 22, p. 100207, Dec. 2022, doi: 10.1016/j.ifacsc.2022.100207.

[12] S. Schölzel, A. Henze, and A.-M. Schreyer, “Numerical analysis of the flow around a speed skydiver,” *European Journal of Mechanics* - B/Fluids, vol. 100, pp. 163–178, Jul. 2023, doi: 10.1016/j.euromechflu.2023.03.006.

[13] C. Wang, Z. Sun, and G. Zhu, “Analysis of flow field and safety of skydiving from the aircraft,” *Aerospace Traffic and Safety*, vol. 2, no. 1, pp. 20–27, Mar. 2025, doi: 10.1016/j.aets.2025.04.001.

[14] Y. Liao, J. Peng, and Y. Gao, “The maximum drop height of high-altitude parachuting based on dynamic and thermodynamic analysis,” *Highlights in Science, Engineering and Technology*, vol. 82, pp. 283–291, Jan. 2024, doi: 10.54097/2857t680.

[15] J. Aiyed, "The kinetics of skydive landings," Master of Science thesis, Department of Kinesiology, California State University, Fullerton., Fullerton, CA, USA, 2023, doi: 10.5281/zenodo.10215370.

[16] M. Ben Slimene, M. A. Khlifi, and I. Tlili, “Advanced mathematical modeling and simulation of high altitude balloons for precision stratospheric data collection,” *Scientific Reports*., vol. 15, no. 1, Dec. 2025, doi: 10.1038/s41598-025-23571-1.

[17] Guide to Reference and Standard Atmosphere Models, AIAA G-003C-2010(2016), American Institute of Aeronautics and Astronautics (AIAA), Reston, VA, USA, 2010.

[18] S. Soniya, “The role of height in the variation of air pressure,” *Journal on Applied and Chemical Physics*, vol. 4, no. 2 June 2025, pp. 35–46, Sep. 2025, doi: 10.46632/jacp/4/2/5.

[19] T. San, S. Polat, C. Cingi, G. Eskiizmir, F. Oghan, and B. Cakir, “Effects of High Altitude on Sleep and Respiratory System and Theirs Adaptations,” *The Scientific World Journal*, vol. 2013, no. 1, Jan. 2013, doi: 10.1155/2013/241569.

[20] A. A. Said, H. P. Mbewe, M. M. Mgimba, H. S. Namanolo, S. M. Rashid, and S. I. Ussi, “Mass Dependent Computational Analysis of Projectile Motion under Quadratic Air Drag Using the Runge-Kutta Method,” *Open Journal of Applied Sciences*, vol. 15, no. 12, pp. 4023–4042, 2025, doi: 10.4236/ojapps.2025.1512260.

[21] P. M. Khudhur, J. Ö. Sigurjónsson, and D. Maghdid, “Modification of the Fourth Order Runge Kutta Method Based on the Contra Harmonic Average,” *Interval: Indonesian Journal of Mathematical Education*, vol. 3, no. 1, pp. 69–81, May 2025, doi: 10.37251/ijome.v3i1.1588.

[22] United States Parachute Association (USPA), "United States Parachute Association – Skydiver Information Manual," USPA, Alexandria, VA, USA, 2023. [Online]. Available: https://www.uspa.org/SIM. [Accessed: Apr. 15, 2026].

[23] O. Eiken, A. Elia, F. Gottschalk, M. Gennser, and R. Ånell, “Decompression strain in parachute jumpmasters during simulated high-altitude missions: a special reference to preoxygenation strategies,” *European Journal of Applied Physiology*., vol. 123, no. 8, pp. 1637–1644, Aug. 2023, doi: 10.1007/s00421-023-05173-9.

[24] S. C. Walpole, D. Prieto-Merino, P. Edwards, J. Cleland, G. Stevens, and I. Roberts, “The weight of nations: An estimation of adult human biomass,” BMC Public Health, vol. 12, no. 1, 2012, doi: 10.1186/1471-2458-12-439.

[25] I. M. S. Abouelhamd, K. Kuga, and K. Ito, “Convective heat transfer and drag coefficients of human body in multiple crowd densities and configurations in semi-outdoor scenarios,” *Building and Environment*., vol. 265, p. 111983, Nov. 2024, doi: 10.1016/j.buildenv.2024.111983.

[26] X. Hou, J. Hu, and Y. Yu, “Numerical Study of Aerodynamic Characteristics of No-Swinging and Free-to-Swing Cross Parachute,” AIAA Journal, vol. 61, no. 11, pp. 5018–5031, Nov. 2023, doi: 10.2514/1.J063034.

[27] D. Johnson, B. Roberts, W. Vaughan, and C. Justus, “Atmospheric Models for Engineering Applications,” in *41st Aerospace Sciences Meeting and Exhibit*, Reston, Virginia: American Institute of Aeronautics and Astronautics, Jan. 2003. doi: 10.2514/6.2003-894.

[28] S. E. D. A. Rehim, N. A. Mostafa, and T. A. Mohamed, “Adjusting the logistic function to develop a more realistic product life cycle model,” *International Journal of Product Lifecycle Management*., vol. 1, no. 1, p. 1, 2021, doi: 10.1504/IJPLM.2021.10039405.

[29] A. E. Parker, “Runge-Kutta 4 (and Other Numerical Methods for ODEs),” 2021. [Online]. Available: https://digitalcommons.ursinus.edu/triumphs_differ/7

[30] F. Condo-Colcha, R. K. Niven, and M. Kramer, “A Shape-Based Model for Drag and Terminal Velocity of Non-Spherical Plastic Particles,” *Water Resources Research*., vol. 62, no. 2, Feb. 2026, doi: 10.1029/2025WR041587.

[31] F. A. Pacala, “Tracking the terminal velocity and energy of a parachutist: A video analysis for Physics classroom experiment,” *Journal of Physics Conference Series*, vol. 2871, no. 1, p. 012011, Oct. 2024, doi: 10.1088/1742-6596/2871/1/012011.

[32] L. Ni, "Study on critical parachute opening speed based on air resistance," *Academic Journal of Engineering and Technology Science*., vol. 7, no. 5, pp. 26–31, Jan. 2024, doi: 10.25236/ajets.2024.070505.

[33] Opale Parachutes, "Rescue parachute – 15 m² / 161 ft²," Opale Parachutes. [Online]. Available: https://www.opale-parachutes.com/gb/parachutes/217-rescue-parachute-15m2-auv-drone-3760245321007.html. [Accessed: Apr. 21, 2026].

[34] Fly Market GmbH & Co. KG, "Erklärung über Bauausführung und Leistung (EBL) / Declaration of Design and Performance (DDP): Ultra Cross 100 (Rettungsgerät/Rescue)," Skyman, Eisenberg, Germany, 2012. [Online]. Available: https://www.skyman.aero/media/ebl-ultra-cross-100.pdf. [Accessed: Apr. 21, 2026]

[35] Sky Country, "SQ reserve parachute by Sky Country," Sky Country, Aug. 27, 2021. [Online]. Available: https://sky-country.com/sq/. [Accessed: Apr. 21, 2026].

[36] NASA Glenn Research Center, "Terminal velocity." [Online]. Available: https://www.grc.nasa.gov/www/k-12/VirtualAero/BottleRocket/airplane/termvr.html. [Accessed: Apr. 10, 2026].